Available online at www.sciencedirect.com

ScienceDirect

Scripta Materialia 93 (2014) 56–59

Scripta MATERIALIA

www.elsevier.com/locate/scriptamat

Hydrogen-induced hardening and softening of Ni–Nb–Zr amorphous alloys: Dependence on the Zr content

Yakai Zhao,[a] In-Chul Choi,[a] Moo-Young Seok,[a] Upadrasta Ramamurty,[b,c] Jin-Yoo Suh[d,*] and Jae-il Jang[a,*]

[a] *Division of Materials Science and Engineering, Hanyang University, Seoul 133-791, Republic of Korea*
[b] *Department of Materials Engineering, Indian Institute of Science, Bangalore 560012, India*
[c] *Center of Excellence for Advanced Materials Research, King Abdulaziz University, Jeddah 21589, Saudi Arabia*
[d] *High Temperature Energy Materials Research Center, Korea Institute of Science and Technology, Seoul 136-791, Republic of Korea*

Received 29 June 2014; accepted 31 August 2014
Available online 18 September 2014

The influence of absorbed hydrogen on the mechanical behavior of a series of Ni–Nb–Zr amorphous metallic ribbons was investigated through nanoindentation experiments. It was revealed that the influence is significantly dependent on Zr content, that is, hydrogen induced softening in relatively low-Zr alloys, whereas hydrogen induced hardening in high-Zr alloys. The results are discussed in terms of the different roles of mobile and immobile hydrogen in the plastic deformation.

Keywords: Hydrogen; Amorphous alloy; Mechanical behavior; Nanoindentation

The science and technology of hydrogen (H) separation is gaining importance for a variety of reasons. A critical component in such technologies, for example in H-powered fuel cells, in the H-permeable membrane, and a number of different options are available for the design engineer. Currently, either Pd or Pd-based alloy membranes are the most popular. However, these are expensive, and alternative materials are being sought actively. One group of potential candidate materials is the Ni–Nb–Zr-based metallic glass (MG) alloy membranes, as their permeability to H is comparable to that of Pd-based ones, but they are much less expensive [1]. In this alloy system, Zr, due to its strong affinity to H, is the key element as it determines the kinetics of H transport [2,3].

An important issue in the context of MG membranes is the H-induced embrittlement [1,3] and efforts to understand the role played by H in the mechanical properties, especially plastic deformation behavior, of MGs are underway. On the one hand, H appears to enhance flow resistance, which is mechanistically similar to that seen in crystalline metals and alloys. On the other hand, few studies report the effects of H-induced softening, such as enhanced shear band density and an enlarged plastic zone in H-containing MGs [4]. Since the free volume content in an MG often determines its plastic response and fracture behavior, and the size of H atoms – being the smallest of all elements – is similar to that of the free volume sites, it is reasonable to expect that the interactions between H in the amorphous structure and the free volume play a vital role in determining the overall response of the H-charged MGs. However, there is disagreement on the changes in free volume associated with hydrogenation. Suh et al.'s [5] positron annihilation lifetime spectroscopy (PALS) measurements on a hydrogenated Zr-based bulk metallic glass (BMG) indicate a decrease in the free volume content upon H-charging, which can explain the increased hardness and decreased fracture toughness. In contrast, Zhou et al.'s [4] PALS studies indicate H-induced free volume expansion, which would mean plastic flow softening upon charging. These contradictory results mandate a systematic study that critically examines the role of H in plastic deformation of amorphous alloys, which is attempted in the present study, wherein nanoindentation is employed to examine a series of MGs with varying Zr contents, both before and after H charging.

MG ribbons that were ~30–60 μm thick were prepared via a conventional melt-spinning technique at Fukuda Metal Foil and Powder Company, Kyoto, Japan. They had the following compositions: $Ni_{45}Nb_{30}Zr_{25}$, $Ni_{33}Nb_{22}Zr_{40}Co_5$, $Ni_{27}Nb_{18}Zr_{50}Co_5$ and $Ni_{35}Nb_{30}Zr_{15}Ti_{10}Fe_5Co_5$ (in at.%), which are considered as candidate materials for MG membranes. These are referred to hereinafter as Zr25, Zr40, Zr50 and Zr15Ti10, respectively. Note that,

* Corresponding authors; e-mail addresses: jinyoo@kist.re.kr; jijang@hanyang.ac.kr

http://dx.doi.org/10.1016/j.scriptamat.2014.08.029
1359-6462/

in Zr15Ti10 alloy, Ti exhibits a strong affinity to H, just like Zr. Gaseous H charging was performed in a Sievert-type apparatus at 300 °C under gas pressure (0.5 MPa) for 3600 s followed by water quenching of the specimen-containing cylinder. Nanoindentation tests were conducted at room temperature using a Nanoindenter-XP (formerly MTS; now Agilent, Oak Ridge, TN, USA) on the roll side surface of the melt-spun ribbons, which were polished with 0.3 μm alumina to a mirror finish. Nanohardness was evaluated with a cube-corner indenter that is sharper than the commonly used Berkovich indenter and produces significantly higher levels of stresses and strains underneath the contact [6,7]. After nanoindentation, indenter impressions were imaged using a field-emission scanning electron microscope (SEM; JSM-340, JEOL Ltd., Tokyo, Japan) and profiled with the aid of an atomic force microscope (AFM; XE-100, Park Systems, Suwon, Korea). In all cases, the maximum depth of penetration (h_{max}, at largest ~2.5 μm) is much less than one-tenth of the ribbon thickness. Hence, the influence of the substrate on the nanoindentation responses could be ignored. All H-charged specimens were tested within 72 h after charging.

The nanoindentation hardness values, H, estimated according to the Oliver–Pharr method [8], are displayed in Figure 1, where representative load–displacement (P–h) curves recorded during nanoindentations are also presented. The plot clearly shows that, for indentations into the uncharged samples, H decreases as the Zr content increases, which is consistent with the increasing interatomic distance with Zr content [9]. A striking result is the dependence of the relative change in H upon hydrogenation on the Zr content in the alloy; H of Zr40 and Zr50 are enhanced whereas Zr15Ti10 and Zr25 become softer (H-induced softening). To illustrate this more vividly, the relative change in hardness due to hydrogenation, ΔH ($=H_C - H_{UC}$, where the subscripts C and UC refer to charged and uncharged alloys, respectively), is plotted as a function of the Zr content in the alloy in the same plot (with open triangle symbols). It is seen that ΔH is ~−2 GPa for Zr15Ti10 and Zr25 and ~+1.5 GPa for the other two alloys.

The H values in Figure 1 were estimated according to the Oliver–Pharr method [8]. To make sure that these values were not affected by the pile-up around the indents [10], we also evaluated the Meyer's hardness, H_M, by measuring the areas of the indentation impressions with the aid of an SEM. Representative images for Zr25 and Zr50 alloys

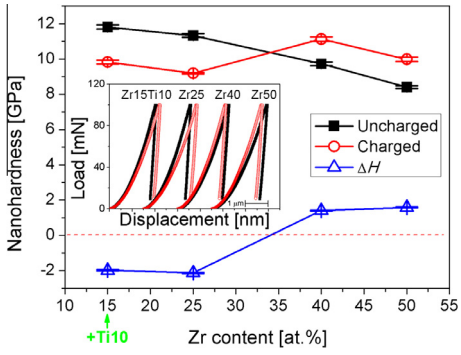

Figure 1. Variation in hardness with Zr content and the H-induced hardness change, ΔH ($=H_C - H_{UC}$). The inset shows representative P–h curves.

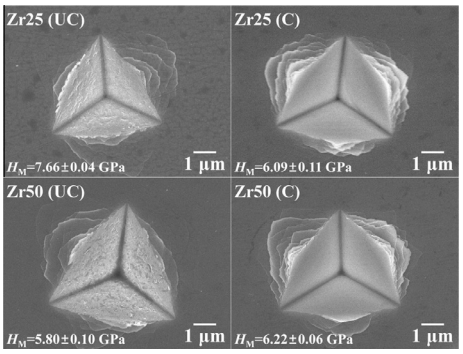

Figure 2. Representative SEM images of nanoindentation impression for Zr25 and Zr50 alloys. UC and C indicate uncharged and charged, respectively.

are shown in Figure 2, where values of H_M ($=P_{max}$/measured impression area [7]) are also provided. These data, which are in general agreement with those plotted in Figure 1, suggest that the observed trends are indeed intrinsic to the material and not experimental artifacts.

The values of ΔH, while intriguing, indicate that the interaction of H with the MG and its consequent influence on plastic deformation are sensitive to the Zr content of the alloy. We surmise that the dual nature of H on the hardness of the MGs, observed in Figure 1, may be closely related to the mobility of H in the amorphous alloys. It has been suggested that the absorbed H in amorphous structure may be partitioned into weakly bound mobile and strongly bound immobile states [1,2]. It has also been conclusively shown [1,11] that H preferentially occupies the polyhedral interstitial sites surrounded by the maximum number of early transition metal atoms (e.g. Ti, Zr) that have a strong affinity with H, and only goes to the other locations when in excess. Thus, it is reasonable to expect the amount of immobile H in higher-Zr amorphous alloys with more Zr-rich sites to be relatively large. Indeed, in a recent study on the same MG systems [12], we have shown that the amount of immobile H scales with the Zr content in the alloy whereas the mobile H amount remains nearly invariant.

From Figure 1, it is seen that both Zr40 and Zr50 exhibit hardening upon H absorption, which is similar to that reported in some other Zr-based BMGs and has been rationalized by Suh et al. [5] – through PALS – as being due to the free volume site occupancy by the absorbed H atoms and, in turn, the reduction in free volume. Typically, these sites are surrounded by hydride-forming elements such as Zr and Ti. A similar conclusion was reached in the nanoindentation studies on a Zr-based BMG [13]. As listed in Table 1, a significant fraction of the H in Zr40 and Zr50 alloys is immobile H, which preferentially occupies those interstitial sites that are mostly surrounded by Zr. In Zr-rich MG systems, hydrogenation can result in the

Table 1. Amount of mobile and immobile H estimated from the data of weight change measurements and H permeation tests [12].

Alloy	Mobile H content (wt.%)	Immobile H content (wt.%)
Zr15Ti10	0.28	0.38
Zr25	0.27	0.57
Zr40	0.28	0.84
Zr50	0.29	1.09

formation of H-rich amorphous clusters [14,15]. This may also occur in the charged Zr40 and Zr50 of the current study; the trapped H is strongly bound with surrounding metallic (mostly Zr) atoms, forming a densely packed structure which has specific chemical and geometrical configurations. This, in turn, results in the constriction of the local atomic movement that would otherwise aid in plastic deformation through the activation of the shear transformation zones (STZs) when the hydrogenated MGs are stressed [14].

While the H-induced hardening discussed above is along the lines expected, the most interesting and counter-intuitive observation of the current study is the H-induced softening in Zr25 and Zr15Ti10. In these cases, mobile H may have a dominant role in assisting plastic deformation due to the relatively low amount of immobile H (see Table 1). To the best of our knowledge, there has been no direct observation of such H-induced softening in MGs in the literature, though a limited amount of indirect evidence exists. For instance, Zhou et al. [4] reported that both the plastic zone size and the free volume in an amorphous Ni–P coating increased with the mobile H concentration, although the Vickers hardness per se did not change significantly after H charging.

When an H atom occupies an interstitial site and the binding between it and its surrounding metallic atoms is weak, it can be considered mobile. One of the main consequences of such occupancy is the increased interatomic distance between metallic atoms surrounding the H due to the inevitable volume expansion by H absorption, which is generally observed in amorphous alloys as well as in crystalline materials [11]. The mobile H acts mostly as a simple "spacer" in the interstitial site, expanding the interatomic spacing without interaction (or strong binding) with surrounding metallic atoms.

Based on this "spacer" concept, three possible mechanisms for mobile H-assisted softening can be proposed, which are schematically illustrated in Figure 3. The first two mechanisms (illustrated in Fig. 3a and b) are based on the two popular mechanisms for explaining the plastic deformation of MGs, viz. the STZ model and local atomic jump model [16], respectively. In Figure 3a, due to the weakened binding force between metallic atoms, STZ activation becomes easier under the applied shear stress,

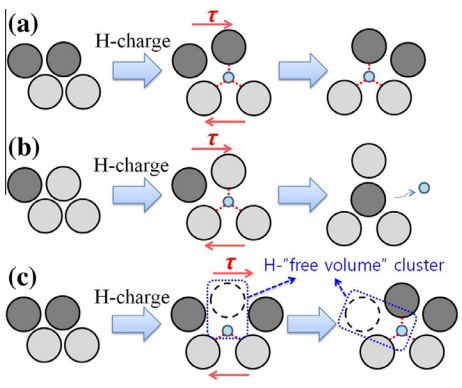

Figure 3. Illustrations of the three possible mechanisms for H-induced softening: (a) H lowering the formation barrier energy of STZ; (b) free volume "creation" by H; and (c) H–"free volume" interaction. Note that these are simplified 2-D illustrations; in reality, an H atom is likely to occupy the tetrahedral site surrounded by atoms with different kinds and sizes.

enhancing plasticity. In Figure 3b, free volume can be created by mobile H atom as follows: during shear, the dark metallic atom in the left side of Figure 3b can move into the dilated space, pushing the H atom out. In this case, the H dilates the space such that the metallic atom can jump into the space with ease. In this sense, the mobile H itself simply plays the role of the free volume for the atomic reconfiguration and can be regarded as the "H-created free volume".

A third possible mechanism, which is somewhat analogous to the H–vacancy interaction in crystalline metals, is illustrated in Figure 3c. In crystalline metals and alloys, the attraction between interstitial H and vacancy is considered to derive a higher level of equilibrium vacancy concentration in H-containing metals than in uncharged metals. This is often referred to as "superabundant vacancy" formation [11,17]. Such vacancies and their clustering were suggested to be the crucial factors influencing the plasticity in H-related failure [18]. In the context of MGs, such interactions must translate into H vs. free volume interactions. Although it is difficult to define "vacancy" in an amorphous structure, if H prefers vacancy to exist nearby, the atomic cluster containing H is likely to have a lower energy barrier for the reconfiguration; in other words, it has a larger free volume. In this regard, the H–vacancy cluster or H–"free volume" cluster can be the predominant mechanism for explaining the observed H-induced softening behavior [19]. It should be noted that the H interacting with the vacancy is a mobile one. Due to their "spacer" effect, the unavoidable volume expansion could be part of the thermodynamic driving force for attracting free volume.

From the SEM images of indents displayed in Figure 2, a noteworthy feature is the variation in the shear band number densities around the nanoindents. In Zr15Ti10 and Zr25, which exhibit H-induced softening, the number of shear bands around the indentations increases with H charging. Note that plasticity enhancement in MGs is usually accompanied by a greater number of closely spaced shear bands [20]. Interestingly, in relatively high-Zr alloys (Zr40 and Zr50), such enhanced densities of shear bands are also observed after H charging, despite the H-induced hardening. This implies that both mobile and immobile H atoms contribute to the plasticity in these alloys, though in different ways. While mobile H can enhance shear banding, as mentioned earlier, immobile H can also enhance it, but in an indirect way; i.e., since heterogeneities (such as inclusions or crystallites) in an amorphous structure can block shear banding and stimulate shear band proliferation [20], the densely packed H-rich structures (where immobile H is trapped) will act as heterogeneities and thus increase the shear band density. Therefore, one may expect that the combined effects by mobile and immobile H will induce the closely spaced shear bands in Zr40 and Zr50 alloys. This hypothesis is supported by additional AFM analyses of the indents made on Zr25 and Zr50, as shown in Figure 4. From the AFM profiles of nanoindentations, the pile-up height is always higher in charged specimens. However, while the average size of each shear offset does not change noticeably in H-charged Zr25, the H-induced size reduction is non-negligible in Zr50. More importantly, the shear offset in the hydrogenated sample (see the arrows in Fig. 4) is smaller for higher Zr content, indicating significant shear band blocking due to immobile H, which, in turn, validates that the densely packed structures formed by immobile H atoms can block the shear bands.

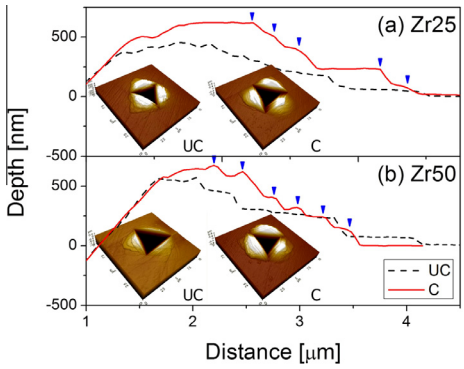

Figure 4. The representative AFM results of cube-corner nanoindentations: (a) Zr25 and (b) Zr50 alloys.

In summary, the effects of H absorption on the strength of four Ni–Nb–Zr amorphous metallic ribbons having various Zr contents were studied. Although the H absorption caused an obvious change in the nanomechanical behavior, the changes for different Zr content alloys appeared differently. While the hardness increased in the Zr40 and Zr50 alloys, a softening behavior was observed in the Zr25 and Zr15Ti10 alloys. The results could be successfully explained by the significant role of H mobility in the mechanical behavior.

The work at Hanyang University was supported in part by the National Research Foundation of Korea (NRF) grant funded by the Korea government (MSIP) (No. 2013R1A1A2A10058551), and in part by the Human Resources Development program of the Korea Institute of Energy Technology Evaluation and Planning (KETEP) grant funded by the Korea government (MOTIE) (No. 20134030200360). The work at KIST was supported by Korea Institute of Science and Technology (2E24692).

[1] M.D. Dolan, N.C. Dave, A.Y. Ilyushechkin, L.D. Morpeth, K.G. McLennan, J. Membr. Sci. 285 (2006) 30.
[2] Y.-I. Wang, J.-Y. Suh, Y.-S. Lee, J.-H. Shim, E. Fleury, Y.W. Cho, S.-U. Koh, J. Membr. Sci. 436 (2013) 195.
[3] S.N. Paglieri, N.K. Pal, M.D. Dolan, S.-M. Kim, W.-M. Chien, J. Lamb, D. Chandra, K.M. Hubbard, D.P. Moore, J. Membr. Sci. 378 (2011) 42.
[4] Q.J. Zhou, J.Y. He, X.P. Hao, W.Y. Chu, L.J. Qiao, Mater. Sci. Eng. A 437 (2006) 356.
[5] D. Suh, P. Asoka-Kumar, R.H. Dauskardt, Acta Mater. 50 (2002) 537.
[6] J.-I. Jang, G.M. Pharr, Acta Mater. 56 (2008) 4458.
[7] I.-C. Choi, Y.-J. Kim, Y.M. Wang, U. Ramamurty, J.-I. Jang, Acta Mater. 61 (2013) 7313.
[8] W.C. Oliver, G.M. Pharr, J. Mater. Res. 7 (1992) 1564.
[9] S.-I. Yamaura, M. Sakuri, M. Hasegawa, K. Wakoh, Y. Shimpo, M. Nishida, H. Kimura, E. Matsubara, A. Inoue, Acta Mater. 53 (2005) 3703.
[10] J.-I. Jang, B.-G. Yoo, Y.-J. Kim, J.-H. Oh, I.-C. Choi, H. Bei, Scr. Mater. 64 (2011) 753.
[11] Y. Fukai, The Metal–Hydrogen System, Springer, Berlin, 2005.
[12] Y. Zhao, I.-C. Choi, M.-Y. Seok, M.-H. Kim, D.-H. Kim, U. Ramamurty, J.-Y. Suh, J.-I. Jang, Acta Mater. 78 (2014) 213.
[13] B.-G. Yoo, J.-H. Oh, Y.-J. Kim, J.-I. Jang, Intermetallics 18 (2010) 1872.
[14] S. Jayalakshmi, K.B. Kim, E. Fleury, J. Alloys Compd. 417 (2006) 195.
[15] X.G. Li, T. Otahara, S. Takahashi, T. Shoji, H.M. Kimura, A. Inoue, J. Alloys Compd. 297 (2000) 303.
[16] C.A. Schuh, T.C. Hufnagel, U. Ramamurty, Acta Mater. 55 (2007) 4067.
[17] N.Z. Carr, R.B. McLellan, Acta Mater. 52 (2004) 3273.
[18] M. Nagumo, N. Nakamura, K. Takai, Metall. Mater. Trans. A 32 (2001) 339.
[19] Y.W. Wang, W.Y. Chu, J.X. Li, X.D. Hui, Y.B. Wang, K.W. Gao, Y.J. Su, L.J. Qiao, Mater. Lett. 58 (2004) 2393.
[20] A.L. Greer, Y.Q. Cheng, E. Ma, Mater. Sci. Eng. R 74 (2013) 71.